JOURNAL OF PROPULSION AND POWER
Vol. 12, No. 2, March–April 1996

Finite Element Analysis of the Scramaccelerator with Hydrogen–Oxygen Combustion

Barry R. Dyne* and Juan C. Heinrich†
University of Arizona, Tucson, Arizona 85715

The Scramaccelerator concept is examined through numerical calculations. A finite element algorithm for inviscid flow calculations is coupled to a chemistry package, and simulations of steady-state detonation waves in a mixture of hydrogen and oxygen are performed for several values of Mach number, projectile-to-tube diameter ratio, mixture equivalence ratio, and fill pressure. The results are expressed in the form of thrust on the projectile. It is concluded that acceleration on the order of 10^5 m²/s on a 200-g projectile could be achieved under the conditions considered.

Introduction

THE Scramaccelerator, a concept derived through recent research in supersonic combustion and detonation, is a method of accelerating a projectile in a tube using gasdynamic techniques. The projectile is fired into a tube by an external mechanism, typically a light-gas gun or ballistic (powder) gun, and shock-induced ignition of the gas mixture in the tube releases energy, producing a pressure increase that further accelerates the projectile. A detailed description of the concepts behind the Scramaccelerator and its important parameters is given by Humphrey.[1] Hertzberg et al.[2] identified five drive modes, covering both supersonic and subsonic combustion. The subsonic drive modes operate in the range of 0.7–3 km/s, above which thrust can no longer be maintained due to thermal choking of the subsonic flow. At higher velocities, acceleration is achieved by maintaining supersonic flow and using an oblique shock to initiate combustion. This supersonic combustion mode Scramaccelerator (Fig. 1) is the subject of the present work.

The objective of this article is to present the results of numerical simulations using a simplified inviscid model, which show that the Scramaccelerator concept is feasible in the sense that thrust is obtained under a variety of conditions when hydrogen and oxygen are used for the fuel–oxidizer mixture. The simulations examine four parameters: 1) Mach number, 2) projectile-to-tube radius, 3) mixture equivalence ratio, and 4) fill pressure. The results are presented in the form of resulting thrust on the projectile.

The numerical simulation of chemically reacting flows presents challenging difficulties because of the strong interactions between the hydrodynamic and chemical processes. The algorithm must provide an oscillation-free representation of the flowfield, since unphysical oscillations may cause the loss or creation of species mass fractions, or even premature ignition, which in turn alters the flow. Another difficulty arises from the disparity in time scales characterizing the flow and the chemistry. The time scales characterizing the flow are usually much larger than those for the chemistry. Shocks of sufficient strength may involve time scales small enough to justify the use of an equilibrium model; however, a finite rate chemistry model is necessary if the algorithm is to cover a wide range of flow regimes including very high velocities and premature ignition of the mixture.

An inviscid flow model with finite rate chemistry is considered here. Viscous effects are important if the temperature in the boundary layer is high enough to cause ignition, or if flow separation occurs, and knowledge of the diffusion properties of each species within the mixture is required. This is therefore only a first step toward a complete reacting flow model. The results obtained with this type of model, however, should approximate the expected thrust of the projectile with reasonable accuracy.

The finite rate chemistry model is necessary to 1) study low-speed operations to determine performance under supersonic combustion conditions when a detonation wave does not occur, 2) account for the possibility of preburning on the nose of the projectile after the bow shock, and 3) study the off-design condition where the detonation interacts with the expansion. In addition, the flow is extremely fast, and appreciable downstream motion may occur during the time of reaction. The gas under consideration is a hydrogen and oxygen mixture, with combustion governed by the 8-reaction, 6-species model used by Yungster.[3,4] Evans and Schexnayder[5] found a 12-species, 25-reaction model to be superior at predicting ignition, but found the 8-reaction model to be as good once ignition had occurred.

Governing Equations

The hydrodynamic governing equations consist of the equations of continuity, momentum, and internal energy, as well as a transport equation for each species within the mixture,

$$\frac{D\rho}{Dt} + \rho\nabla\cdot\boldsymbol{u} = 0 \tag{1}$$

$$\rho\frac{D\boldsymbol{u}}{Dt} = -\nabla p \tag{2}$$

$$\rho\frac{De}{Dt} = -p\nabla\cdot\boldsymbol{u} \tag{3}$$

$$\rho\frac{Dc_i}{Dt} = \dot{w}_i \qquad i = 1, 2, \ldots, ns-1 \tag{4}$$

where ρ is the density, $\boldsymbol{u}$ is the velocity vector, p is pressure, e is the internal energy, $c_i \equiv \rho_i/\rho$ is the mass fraction of species

Presented as Paper 93-0745 at the AIAA 31st Aerospace Sciences Meeting and Exhibit, Reno, NV, Jan. 11–14, 1993; received Feb. 8, 1993; revision received June 15, 1995; accepted for publication Aug. 30, 1995.

*Graduate Research Assistant, Department of Aerospace and Mechanical Engineering; currently Research Scientist, Tanner Research, Inc., 180 North Vinedo Avenue, Pasadena, CA. Member AIAA.

†Professor, Department of Aerospace and Mechanical Engineering.

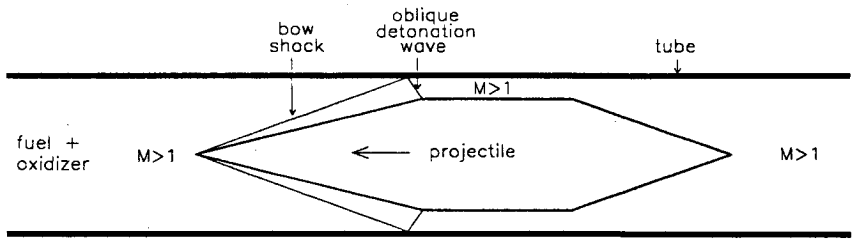

Fig. 1 Oblique detonation wave Scramaccelerator.

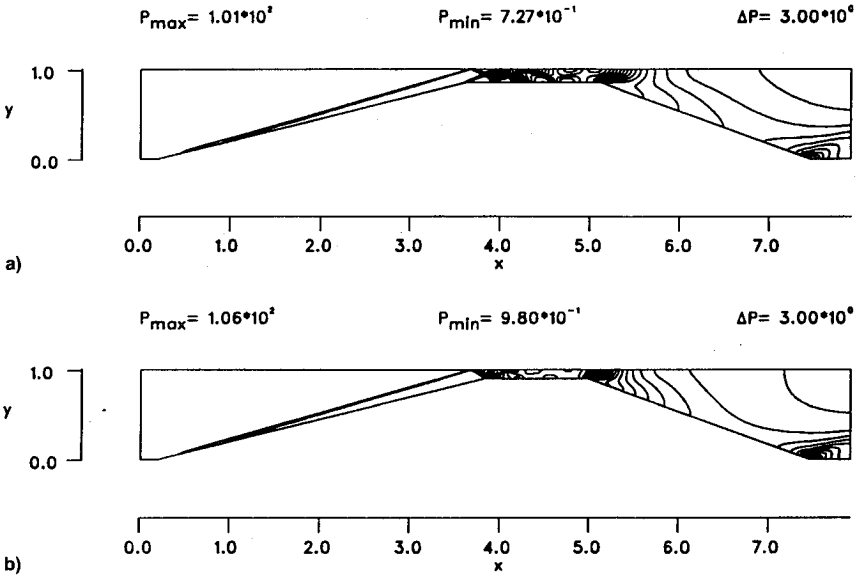

Fig. 2 Pressure contours for a Mach 8 reacting flow of $O_2 + 2H_2$ through a Scramaccelerator; r = a) 0.85 and b) 0.90.

i, $\dot{w}_i$ is the rate of change in ρ_i due to chemical reaction, and ns is the number of species. The mass fraction of species ns is calculated from the conservation equation $\Sigma_{i=1}^{ns} c_i = 1$. The equation of state is

$$p = \rho RT \tag{5}$$

where R now varies with the composition of the mixture and is given by $R = \mathcal{R} \Sigma_{i=1}^{ns} c_i/\mathcal{M}_i$, where $\mathcal{R}$ is the universal gas constant and $\mathcal{M}_i$ is the molecular weight of species i. Following Pratt,[6,7] the chemical reactions are written as a set of nr elementary reactions of the form

$$\sum_{i=1}^{ns} \nu'_{ij} X_i \rightleftharpoons \sum_{i=1}^{ns} \nu''_{ij} X_i \qquad j = 1, 2, \ldots, nr \tag{6}$$

where ν'_{ij} and ν''_{ij} are the stoichiometric coefficients of species i for reaction j as reactants and products, respectively, and X_i represents species i. The net reaction rate of species X_i, taken from Pratt,[6,7] is given by the empirical formulation

$$\frac{d[X_i]}{dt} = \sum_{i=1}^{nr} \left\{ (\nu''_{ij} - \nu'_{ij}) \times \left(k_{+j} \prod_{k=1}^{ns} [X_k]^{\nu'_{kj}} - k_{-j} \prod_{k=1}^{ns} [X_k]^{\nu''_{kj}} \right) \right\} \tag{7}$$

where $[X_i] \equiv \rho c_i/\mathcal{M}_i$ is the concentration of species i and is related to $\dot{w}_i$ by $d[X_i]/dt = \dot{w}_i/\mathcal{M}_i$. The forward and reverse reaction rate constants are given by the Arrhenius expression

$$k_{\pm j} = 10^{B_{\pm j}} T^{N_{\pm j}} \exp(-T_{\pm j}/T) \tag{8}$$

where $B_{\pm j}$, $N_{\pm j}$, and $T_{\pm j}$ are constants for reaction j.

The fuel–oxidizer mixture used in this work is a hydrogen–oxygen mixture with six reacting species (H, H_2, O, O_2, OH, and H_2O), plus an inert species M that acts as a collision partner with unit efficiency. The model, as written in general form in Eq. (6), is given by the following eight reactions:

$$H + O_2 \rightleftharpoons OH + O$$

$$O + H_2 \rightleftharpoons OH + H$$

$$H_2 + OH \rightleftharpoons H + H_2O$$

$$2OH \rightleftharpoons O + H_2O$$

$$H_2 + M \rightleftharpoons 2H + M$$

$$H_2O + M \rightleftharpoons OH + H + M$$

$$OH + M \rightleftharpoons O + H + M$$

$$O_2 + M \rightleftharpoons 2O + M$$

Numerical Method

The hydrodynamic equations are solved via a finite element formulation in which a Petrov–Galerkin method and selective reduced integration have been used to eliminate spatial oscillations. Velocity, density, and energy have been discretized with bilinear quadrilateral isoparametric elements, and pressure is approximated with piecewise-constant functions. Scramaccelerator simulations are performed in an axisymmetric for-

mulation, where the weak form of the governing equations may be written as

$$\left[\int_\Omega \left(N_i \sum_{j=1}^{nn} N_j\right) d\Omega\right] \frac{\partial \rho_i}{\partial t} = -\int_\Omega W_i \left(u^h \frac{\partial \rho^h}{\partial r} + v^h \frac{\partial \rho^h}{\partial z}\right) d\Omega - \int_\Omega N_i \rho^h \left(\frac{1}{r}\frac{\partial r u^h}{\partial r} + \frac{\partial v^h}{\partial z}\right) d\Omega \quad (9)$$

$$\left[\int_\Omega \left(\rho^h N_i \sum_{j=1}^{nn} N_j\right) d\Omega\right] \frac{\partial u_i}{\partial t} = -\int_\Omega W_i \left(u^h \frac{\partial u^h}{\partial r} + v^h \frac{\partial u^h}{\partial z}\right) d\Omega + \frac{1}{\gamma M^2}\int_\Omega \frac{\partial N_i}{\partial r} p^h \, d\Omega - \frac{1}{\gamma M^2}\int_\Gamma N^i p^h \, d\Gamma \quad (10)$$

$$\left[\int_\Omega \left(\rho^h N_i \sum_{j=1}^{nn} N_j\right) d\Omega\right] \frac{\partial v_i}{\partial t} = -\int_\Omega W_i \left(u^h \frac{\partial v^h}{\partial r} + v^h \frac{\partial v^h}{\partial z}\right) d\Omega + \frac{1}{\gamma M^2}\int_\Omega \frac{\partial N_i}{\partial z} p^h \, d\Omega - \frac{1}{\gamma M^2}\int_\Gamma N_i p^h \, d\Gamma \quad (11)$$

$$\left[\int_\Omega \left(\rho^h N_i \sum_{j=1}^{nn} N_j\right) d\Omega\right] \frac{\partial e_i}{\partial t} = -\int_\Omega W_i \left(u^h \frac{\partial e^h}{\partial r} + v^h \frac{\partial e^h}{\partial z}\right) d\Omega + \frac{1}{\gamma M^2}\int_\Omega N_i p^h \left(\frac{1}{r}\frac{\partial r u^h}{\partial r} + \frac{\partial v^h}{\partial z}\right) d\Omega \quad (12)$$

$$\int_\Omega \left(\rho^h N_i \sum_{j=1}^{nn} N_j\right) d\Omega \frac{\partial c_i^h}{\partial t} = -\int_\Omega W_i \left(u_h \frac{\partial c_i^h}{\partial r} + v_h \frac{\partial c_i^h}{\partial z}\right) d\Omega + \int_\Omega N_i \dot{w}_i \, d\Omega \quad (13)$$

where $\alpha^h = \sum_{i=1}^{nn} N_i \alpha_i$ for $\alpha = \rho, u, v, e, c_i, \dot{w}_i$ are the discretized dependent variables; and N_i are the bilinear shape functions. The subscript i denotes the value of the function at node i, and nn is the number of nodes.

The pressure p^h is constant over each element and must be calculated using a consistent piecewise constant representation for the density and internal energy. Reduced one-point integration, denoted by $\oint$, is used to calculate the terms containing the pressure and in the continuity equation [Eq. (9)]. The reasons for this have been explained in Ref. 9. In the rest of the integrals, a 2 × 2 Gauss quadrature is used. The right-hand side of Eqs. (9–13) contains a diagonal lumped mass matrix.

The Petrov–Galerkin weighting functions W_i are given by[8,9]

$$W_i = N_i + (h_i/2U)\boldsymbol{u}\cdot\nabla N_i \quad (14)$$

where $U = |\sqrt{u^2 + v^2}|$ and h_i is an element length defined by Heinrich and Yu.[10]

The chemistry calculations are performed using the program CFDK (computational fluid dynamics kinetics) by Radhakrishnan and Pratt,[11] which is designed to perform chemical calculations in a reacting flow simulation by the method of fractional steps (or operator splitting). Hence, one iterates a flow step with frozen chemistry and a chemistry step with frozen flow. The chemistry solution step consists of a loop over each node in the domain, in which CFDK takes fluid properties and the time step from the previous flow step and integrates the chemistry equations, subdividing the time step as needed for stability. Reacted properties are returned and the next node is considered. Iteration between flow and chemistry solutions continues until convergence. To determine when the calculations had reached a steady state, the partial derivatives with respect to time for each of the physical quantities were evaluated at the nodes. Steady state was determined to occur after the derivatives remained below a predetermined value ε for a time equivalent to 0.01 s. In the present calculations, $\varepsilon = 10^{-8}$ in nondimensional units.

Examples

Extensive code verification has been performed for nonreacting flows at both high and low Mach numbers. A full account of these tests is given by Dyne.[12]

For flow with chemical reactions, the case of a steady oblique detonation wave for flow at Mach number 7 over a 20-deg two-dimensional wedge was considered. The results were compared with those from an analytical model for two-dimensional oblique detonation waves by Pratt et al.,[13] in which a term for the energy release due to combustion is explicitly added to the energy equation. Upstream conditions are at a pressure of 50 atm and a temperature of 300 K. The mixture is a stoichiometric oxygen–hydrogen combination. Table 1 shows a comparison of the calculated downstream properties with those of the analytical model. The cold flow solution for Mach 7 flow over a 20-deg wedge yields a shock angle of 26.7 deg, whereas the detonation wave has an angle of 54.5 deg, showing that the heat release due to combustion significantly modifies the shock angle. The largest difference between the models is for the pressure rates, and this is less than 5%.

Calculations for the Scramaccelerator were performed in an axisymmetric geometry on a configuration with a nose cone angle of 14 deg, a nozzle cone angle of 20 deg, and a tube radius of 2.0 cm. Two projectile-to-tube ratios, $r = 0.85$ and $r = 0.90$, were used. For both cases, the mesh contained 35 nodes, equally distributed in the radial direction at every cross section perpendicular to the z axis, and 250 nodes in the axial direction, clustered more densely near the detonation region. The calculations were performed on a fixed mesh. Steady-state results were calculated via the transient algorithm, which should capture physical instabilities if they occur. Detonation simulations are sensitive to mesh refinement and it was observed that convergence could not be obtained if the finite element grids were not sufficiently refined in the detonation region. For grids that were not fine enough, the detonation wave would not stabilize to a fixed location. Computations were carried out using several mesh resolutions in both the axial and radial directions. Results presented here are for the finest mesh used. In these calculations, the detonation wave and reaction zone are captured within three elements. The steady-state results should provide a good approximation to a real accelerating projectile because the flow adjusts faster than significant increases in projectile velocity.[14] Mach numbers of 7, 8, and 9, tube fill pressures of 20, 50, and 100 atm, and hydrogen–oxygen equivalence ratios of 0.5, 1.0, and 2.0 are considered. The overdrive ratios for these calculations vary between 1.35–1.73; no instabilities were observed for the lowest value of 1.35. We expect that the time-dependent algorithm would capture this behavior if the detonations were unstable. We should also note that an equilibrium chemistry model would be sufficient for the examples presented here; however, our objective is to develop a general model that is valid over a wide range of operating conditions, which include those for which finite rate chemistry is required. The examples presented here are the first of a continuing developmental effort.

Table 1 Comparison of detonation wave properties[a]

Source	P_1/P_2	T_1/T_2	M_2
Calculated	25.3	15.0	1.50
Pratt et al.[12]	24.2	15.2	1.55
Δ%	4.67	1.33	3.22

[a]Subscripts 1 and 2 denote quantities upstream and downstream of the detonation wave, respectively.

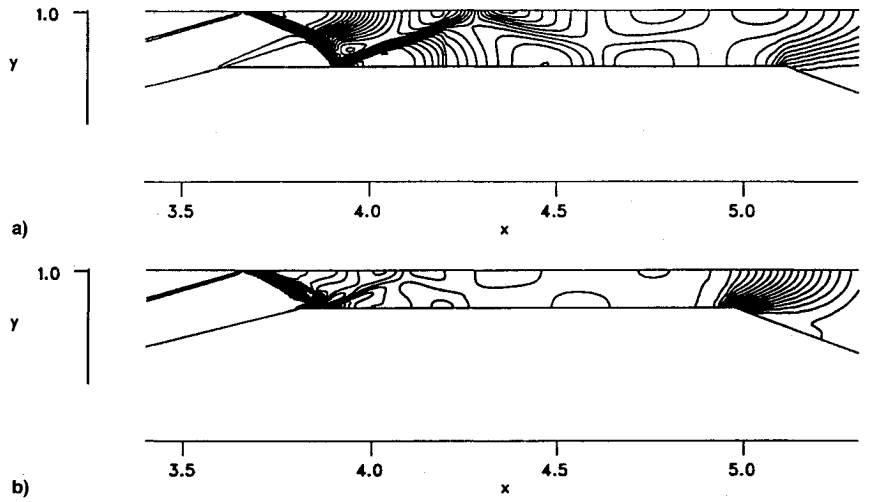

Fig. 3 Expanded view of the detonation region for a Mach 8 flow of O_2 + $2H_2$ through Scramaccelerator; r = a) 0.85 and b) 0.90.

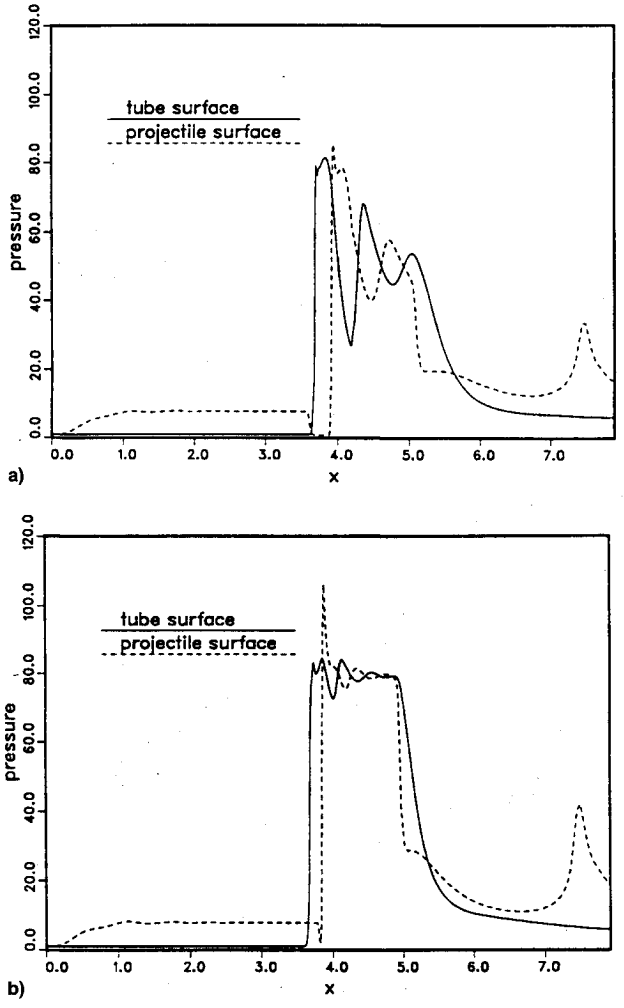

Fig. 4 Pressure along projectile and tube surfaces for a Mach 8 reacting flow of O_2 + $2H_2$ through a Scramaccelerator; r = a) 0.85 and b) 0.90.

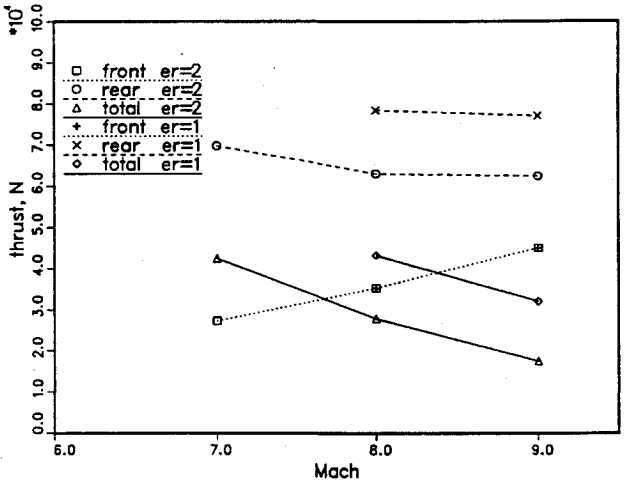

Fig. 5 Thrust vs Mach number for reacting flow through a Scramaccelerator; r = 0.085.

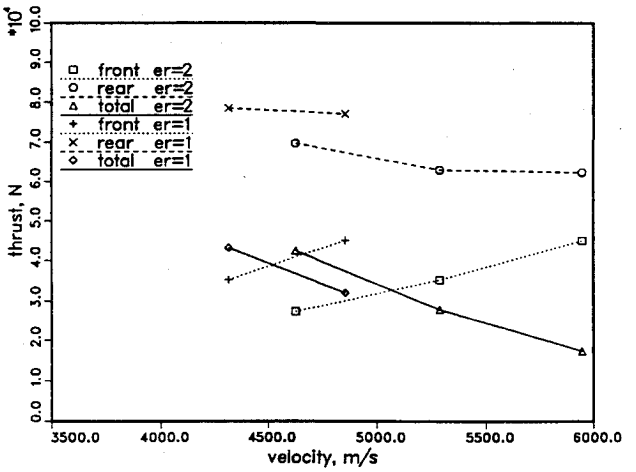

Fig. 6 Thrust vs velocity for reacting flow through a Scramaccelerator; r = 0.085.

Figure 2 shows the pressure for calculations at r = 0.85 and 0.90 with flow at M = 8, for a stoichiometric gas mixture O_2 + $2H_2$, at a tube fill pressure of 50 atm. Expanded views of the detonation region are shown in Fig. 3. For the case of r = 0.85, the shock strikes the tube wall approximately above the shoulder, and the detonation wave hits the projectile downstream of the shoulder, resulting in reflection in the gap. Interaction with the shoulder is seen to curve the detonation wave toward the shoulder. For the r = 0.90 case, the detonation wave strikes almost at the shoulder, virtually eliminating reflections in the gap and resulting in pressure and temperatures that are close to uniform. The presence of a detonation wave is further verified by the calculated concentration of H_2O, which is zero upstream of the detonation wave, increases sharply over a thin layer behind the shock where full com-

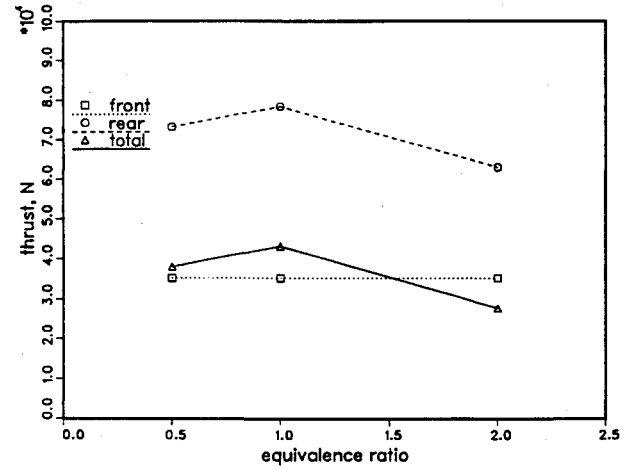

Fig. 7 Thrust vs equivalence ratio for a Mach 8 reacting flow through a Scramaccelerator; $r = 0.085$.

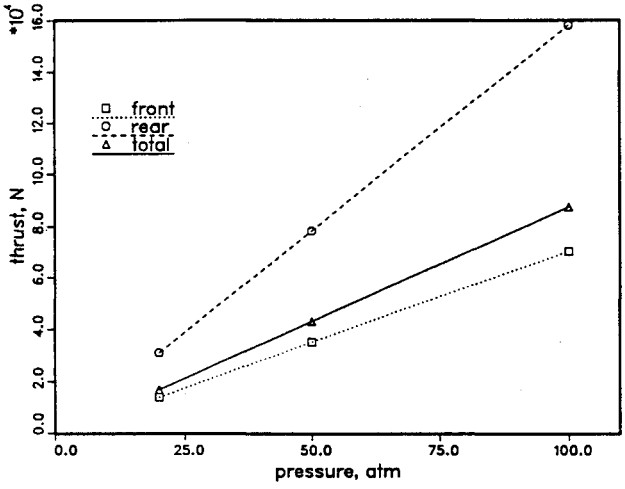

Fig. 8 Thrust vs tube fill pressure for a Mach 8 reacting flow through a Scramaccelerator; $r = 0.085$.

bustion occurs, and remains uniform on the downstream side of the layer.

Optimal conditions occur when the detonation wave strikes at the shoulder, avoiding losses due to reflections. The $r = 0.90$ case shows a better performance than the 0.85 case. Figure 4 shows pressure along the projectile and tube surfaces for the two gaps considered. The shock reflections can be observed in the $r = 0.85$ case, while a more uniform pressure behind the detonation curve and greater pressure on the rear results for the $r = 0.90$ case. Significant increases in thrust may be achieved by contouring the nozzle region to expand the gas more gradually.[15]

Thrust on the projectile is calculated by integrating the pressure on the surface and subtracting the force on the front from the force on the rear. Thrust vs Mach number and thrust vs projectile velocity are shown in Figs. 5 and 6 for equivalence ratios of 1.0 and 2.0 at a tube fill pressure of 50 atm and $r = 0.85$. Forces on the front and rear are shown by the dotted and dashed lines, respectively, and the solid curves are the total thrust. It is important to notice the decrease in thrust with increasing velocity, due to both an increase in force on the front of the projectile and a decrease in force on the rear. Considering a constant Mach number, thus eliminating differences on the projectile front, we see that the stoichiometric mixture provides a greater thrust than the fuel-rich mixture. If we look at a constant velocity, however, the rich mixture provides a greater thrust than the stoichiometric mixture. The difference is due to the difference in Mach numbers. Figure 7 gives thrust vs equivalence ratio for the $r = 0.85$ projectile at Mach 8 and 50 atm fill pressure, showing a maximum thrust for the stoichiometric mixture. Finally, we observe a linear relationship between thrust and fill pressure in Fig. 8, indicating that one would want to use as high a pressure as possible, the only limitation being structural considerations.

Conclusions

A finite element flow solver has been successfully coupled with the chemical reaction program CFDK, providing the capability of computing chemically reacting compressible flows in complex geometries. Scramaccelerator computations were performed at various projectile-to-tube ratios, Mach numbers, mixture equivalence ratios, and tube fill pressures.

The results shown in Figs. 5–8 indicate that the thrust obtained for the worst case is 1.8×10^4 N. For a 200-g projectile, this translates into a worst-case acceleration of 9×10^4 m/s^2. The best performance results in a thrust of 8.2×10^4 N (Fig. 8), with an acceleration of 4.1×10^5 m/s^2 for a 200-g projectile. These numbers provide strong evidence of the viability of the Scramaccelerator concept. The robustness of the numerical model has also been tested in a geometry with very high compression and expansion ratios.

References

[1]Humphrey, J. W., "Parametric Study of an ODW Scramaccelerator for Hypersonic Test Facilities," AIAA Paper 90-2470, July 1990.

[2]Hertzberg, A., Bruckner, A. P., and Bogdanoff, D. W., "Ram Accelerator: A New Chemical Method for Accelerating Projectiles to Ultrahigh Velocities," *AIAA Journal*, Vol. 26, No. 2, 1988, pp. 195–203.

[3]Yungster, S., "Numerical Study of Shock-Wave/Boundary Layer Interactions in Premixed Hydrogen-Air Hypersonic Flows," AIAA Paper 91-0413, Jan. 1991.

[4]Yungster, S., Eberhardt, S., and Bruckner, A. P., "Numerical Simulation of Hypervelocity Projectiles in Detonable Gases," *AIAA Journal*, Vol. 29, No. 2, 1991, pp. 187–199.

[5]Evans, J. S., and Schexnayder, C. J., "Influence of Chemical Kinetics and Unmixedness on Burning in Supersonic Hydrogen Flames," *AIAA Journal*, Vol. 18, No. 2, 1980, pp. 188–193.

[6]Pratt, D. T., and Woomeck, J. J., "CREK: A Computer Program for Calculation of Combustion Reaction Equilibrium and Kinetics in Laminar or Turbulent Flows," Washington State Univ., WSU-ME-TEL-76-1, Pullman, WA, 1976.

[7]Pratt, D. T., "Calculation of Chemically Reacting Flows with Complex Chemistry," *Studies in Convection*, edited by B. E. Lauder, Vol. 2, Academic, London, 1977.

[8]Brueckner, F. P., and Heinrich, J. C., "Petrov-Galerkin Finite Element Model for Compressible Flows," *International Journal for Numerical Methods in Engineering*, Vol. 32, No. 2, 1991, pp. 255–274.

[9]Dyne, B. R., and Heinrich, J. C., "Physically Correct Penalty-Like Formulation for Accurate Pressure Calculation in Finite Element Algorithms of the Navier-Stokes Equations," *International Journal for Numerical Methods in Engineering*, Vol. 36, No. 2, 1993, pp. 3883–3902.

[10]Heinrich, J. C., and Yu, C.-C., "Finite Element Simulation of Buoyancy-Driven Flows with Emphasis on Natural Convection in a Horizontal Circular Cylinder," *Computer Methods and Applications in Mechanical Engineering*, Vol. 69, No. 1, 1988, pp. 1–27.

[11]Radhakrishnan, K., and Pratt, D. T., "Fast Algorithm for Calculating Chemical Kinetics in Turbulent Reacting Flow," *Combustion Science and Technology*, Vol. 58, Nos. 1–3, 1988, pp. 155–176.

[12]Dyne, B. R., "Finite Element Analysis of Incompressible, Compressible, and Chemically Reacting Flows, with an Emphasis on the Pressure Approximation," Ph.D. Dissertation, Univ. of Arizona, Tucson, AZ, 1992.

[13]Pratt, D. T., Humphrey, J. W., and Glenn, D. E., "Morphology of a Standing Oblique Detonation Wave," *Journal of Propulsion and Power*, Vol. 7, No. 5, 1991, pp. 837–845.

[14]Brackett, D. C., and Bogdanoff, D. W., "Computational Investigation of Oblique Detonation Ramjet-in-Tube Concept," *Journal of Propulsion and Power*, Vol. 5, No. 3, 1989, pp. 276–281.

[15]Brueckner, F. P., "Finite Element Analysis of High-Speed Flows with Application to the Ram Accelerator Concept," Ph.D. Dissertation, Univ. of Arizona, Tucson, AZ, 1991.